Mahmoud Mostafa*, Christopher Varela and Edwin Zondervan

2 Optimization of electrolysis and carbon capture processes for sustainable production of chemicals through Power-to-X

Abstract: This contribution presents the modelling and optimization strategy of the key intermediate processes in Power-to-X: water electrolysis and carbon capture. While the water electrolysis process is set to maximize the profit provided market data, the control structure in the capture process allows the production of the stoichiometric amount of carbon dioxide for further processing to methanol. The flexible operation of electrolyzers allowed efficient conversion of renewable energy into hydrogen with minimum grid compensation (around 4%). Furthermore, the capture process showed a favourable response to the fluctuating demand of CO_2, with deviations lower than 1% over the simulated period. This optimization strategy represents a viable option for Power-to-X processes to cope with the fluctuations of volatile renewable energy.

Keywords: alkaline water electrolysis; carbon capture; hydrogen; Power-to-X; renewables.

2.1 Introduction

The volatility of renewable energy sources (RES) poses a major challenge for the energy transition, especially wind and photovoltaic due to variable weather conditions. Curtailment of renewable energy rose to about 6146 GWh during 2020 in Germany [1]. The energy loss will increase with the forthcoming expansion of RES. Thus, it is essential to provide efficient storage of renewable electricity, which may include thermal, mechanical, electrical, or electrochemical systems. The electrochemical storage category comprises, in addition to batteries, chemical energy carriers such as hydrogen, methane or liquid fuels [2]. This storage pathway, also known as Power-to-X

***Corresponding author: Mahmoud Mostafa**, Laboratory of Process Systems Engineering, University of Bremen, Leobener Str. 6, 28359 Bremen, Germany; and Department of Chemical Engineering, Twente University, 7522 NB Enschede, The Netherlands, E-mail: mmostafa@uni-bremen.de. https://orcid.org/0000-0001-9030-6158

Christopher Varela, Laboratory of Process Systems Engineering, University of Bremen, Leobener Str. 6, 28359 Bremen, Germany; Department of Chemical Engineering, Twente University, 7522 NB Enschede, The Netherlands; and Facultad de Ciencias Naturales y Matemáticas, Escuela Superior Politécnica del Litoral, ESPOL, Campus Gustavo Galindo Km. 30.5 Vía Perimetral, Guayaquil, P.O. Box 09-01-5863, Ecuador

Edwin Zondervan, Department of Chemical Engineering, Twente University, 7522 NB Enschede, The Netherlands

As per De Gruyter's policy this article has previously been published in the journal Physical Sciences Reviews. Please cite as: M. Mostafa, C. Varela and E. Zondervan "Optimization of electrolysis and carbon capture processes for sustainable production of chemicals through Power-to-X" *Physical Sciences Reviews* [Online] 2022. DOI: 10.1515/psr-2020-0056 | https://doi.org/10.1515/9783110705201-002

(P2X), offers the opportunity to integrate electricity generation with industrial processes and mobility, while improving the grid stability (electrolysis acts as a fast-negative energy balancing unit when the grid is overloaded from RES) and promoting higher penetrations of RES in the energy mix.

The main components of a P2X system are the electrolytic production of hydrogen and carbon capture process, as shown in Figure 2.1. With hydrogen and carbon dioxide as raw materials it is possible to synthesize a wide range of products, namely methane, methanol, fuels, etc.

Previous work is based on modelling water electrolysis and carbon capture for continuous processes [3, 4]. Hqowever, the focus of this work is to present modelling and optimization strategies for water electrolysis and carbon capture which include the time domain due to the energy fluctuations. This leads to the formulation of discrete-event and dynamic models, as well as the integration of those models to find the optimal operation of a case study.

2.2 Process modelling and optimization

2.2.1 Dynamic carbon capture

The dynamic carbon capture model allows us to study the transient operation of the carbon capture process, having minimum control and assuming no storage facility for

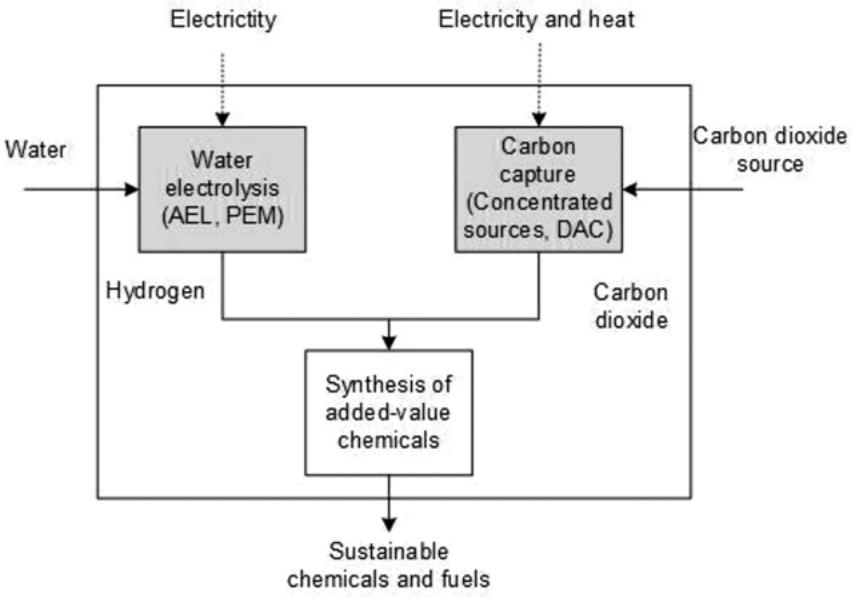

Figure 2.1: Power-to-X concept with water electrolysis and carbon capture as the key process stages.

the solvent. The main goal of the simulated process model is to track the parallel hydrogen production, capturing the stoichiometric required carbon dioxide stream that acts as feed to a methanol reactor within a P-to-X plant [5].

2.2.1.1 Model development

The simulated steady-state model enables us to set the control basis for dynamic simulation; additional data (sump height/diameter, pumps, valves) are required for the steady state simulation to be exported into dynamic mode. Further details on the design and simulation of the carbon capture model are found in the study by Mostafa et al. [5]. The process scheme of the various stages involved in a typical carbon capture stage is shown in Figure 2.2. MEA solvent is chosen for the simulated model, where it reacts with the CO_2 component exothermically. The dynamic model along with the proposed control system will provide us with deeper insight on how the process behaves when operated in transient mode. Disturbances can either be operator-induced disturbances such as changing the flue gas flow rate or the capture rate set point; or uncontrolled disturbances due to weather conditions, for instance heavy rain hitting the side of the column. For optimal process performance, disturbances have to be accounted for in the design, where changes on the operating variables are then made to achieve the fastest stabilising time back to the set point. Changes are made within the allowable process variables set by unit operation and environmental policies.

As the carbon capture plant lies within a P-to-X facility, changes could occur in the final product demand and cost meaning that the process must be flexible enough to cope with the fluctuating objectives. A study by Oates et al. [6] focused on the profitability of the power plant when equipped with a carbon capture unit, proving that

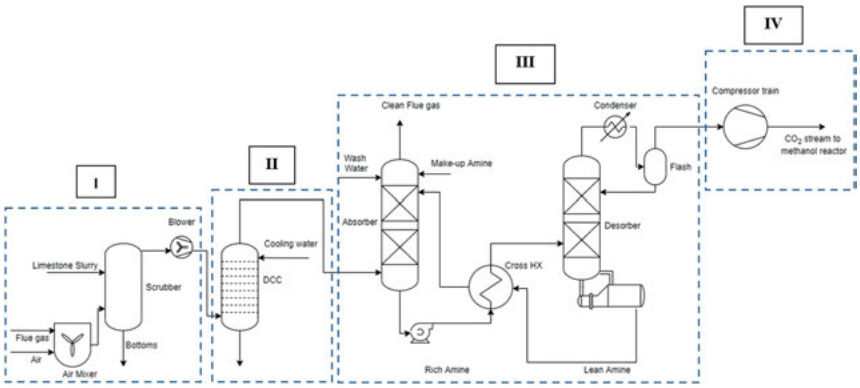

Figure 2.2: Process flow diagram of CO_2 capture plant (I: desulfurization unit, II: flue gas cooling (DCC), III: absorption/desorption stage, IV: CO_2 compression stage).

the process is profitable under environmental policies. The control strategy is an important aspect in the dynamic operation, process control ensures safe operation within the specified constraints. The tank level or vessel pressure for example should not exceed the maximum allowable values set by the operator.

Disturbances cause deviation in the output conditions (temperature, pressure, flow rate) from the initial steady state, those disturbances should be suppressed if no new state is desired. If the disturbance is induced such as reduction in the flue gas flue rate with the objective of reducing the amount of CO_2 captured, then the controllers act to restore the unit conditions back to the set point to accommodate this new state. Both the power and the speed of the control loop are considered when setting up the control strategy. Power of control refers to the impact the correcting variable has on the controlled variable, where the control loop has an appropriate impact on the process. On the other hand, the speed of the control loop refers to the dynamic impact of the loop on the process. It is limited by the dead time in the control loop consisting of the correcting device, the actual process and the measuring device [5].

The control scheme applied would enable the operator to achieve the desired objectives in terms of stream specifications. In our specific case study, the carbon capture plant should be flexible enough to capture a changing amount of CO_2 from the feed flue gas. The final concentrated CO_2 stream should have a specific mass fraction according to the purity requirements set by the methanol reactor that follows the CC stage. In actual operation, the stream purity might be complicated and expensive to measure directly online, thus an inferential control solution is applied. Easily measured variables such as the condenser temperature can be controlled to maintain a desired stream purity condition. Inferential control saves the cost of an online CO_2 analyzer as it would be replaced by an inexpensive thermocouple. Several factors need to be taken into consideration in order to achieve the mentioned objectives:

1. **Absorber capture rate:** Using a PI controller the amount of CO_2 captured from the feed flue gas is controlled by manipulating the lean amine flow rate.
2. **Flue gas exit pressure:** The pressure is maintained by manipulating the flow rate of the gas stream exiting the absorber.
3. **Absorber sump level:** The solvent level is measured at the bottom of the absorber and controlled by manipulating the exiting rich amine flow rate.
4. **CO_2 stream temperature:** The condenser duty is manipulated to control the concentrated CO_2 stream temperature.
5. **Stripper output stream pressure:** A control valve manipulates the exiting CO_2 stream flowrate to control the pressure.
6. **Stripper sump level:** Similar control mechanism to the absorber sump level control.
7. **Stripper operating temperature:** Through manipulating the reboiler duty (steam flowrate) the stripper temperature is maintained, thus ensuring a constant lean loading of 0.2.

An initial control strategy to control the absorber temperature was through manipulating the washing section flowrate. The results indicated a low power of control, where the correcting variable (washing section flowrate) had no impact on the controlled variable (absorber temperature). Through controlling the capture rate and the operating conditions of the absorber and desorber columns, the carbon dioxide flowrate, purity, pressure, and temperature were controlled and monitored throughout the entire dynamic operation. The type of controllers and tuned up parameter values are listed in Table 2.1:

2.2.2 Alkaline water electrolysis

Alkaline water electrolysis (AEL) comprises electrolysis stacks, gas-liquid separators, deoxidizers, and ancillary equipment for heat and flow management. An integrated control guarantees both safe operation and product quality [7]. AEL stacks usually work at temperature between 50 and 80 °C, pressure from atmospheric to 30 bar, current density in the range of 200–4500 A/m^2-cell, and electrolyte concentration between 20 and 40 wt% KOH. With the treatment section, the purity of hydrogen can be up to 99.9 v/v%. [2, 8].

2.2.2.1 AEL stack model

The stack model is constructed by implementing a non-linear program (NLP) to estimate the parameters defined in the model proposed by Ulleberg [9], considering a large-scale electrolyzer [10]. The NLP-constraints correspond to the stack model evaluated at maximum power load, with a current density of 3500 A/m^2, and minimum load of 10% with respect to the nominal power load. The estimated parameters are listed in, while the performance of the proposed stack is shown in Figure 2.3. Furthermore, the peripheral load is estimated from the difference between the maximum load of the stacks and the module power consumption.

2.2.2.2 AEL scheduling model

This model has been constructed as a mixed-integer linear program (MILP) that allows minimizing the production cost of the facility [11]. The model includes operating states and transitions of AEL stacks Table 2.2, cost terms to the objective function, and a set of heuristic rules to constrain the operation to physical and technical limitations.

The main characteristics to consider related to operation under load changes are load range, ramp up- and down rate, and start-up and shutdown time. The load range of alkaline water electrolyzers is about 10–100% of the nominal capacity. This boundary cannot be violated due to safety reasons. The ramp up-and down rates do not present a limitation for the case study due to the difference in the time scale. The main

Table 2.1: The absorber and desorber tuned controller parameters.

Unit	Controller type	Controlled variable (PV)	Manipulated variable (OP)	Maximum value	Gain (%/%)	Integral time (min)
Absorber	Pressure controller	Flue gas pressure, bar	Flue gas flow rate	3.6	20	12
	Sump level controller	Sump height, m	Rich amine flow rate	7.35	0.187	85
	Capture rate	CO_2 exit flow rate, kg/h	Lean amine flow rate	14,711	0.635	2.17
Stripper	Pressure controller	Exit stream pressure, bar	CO_2 stream flow rate	4	20	12
	Sump level controller	Sump height, m	Lean amine flow rate	6.16	0.136	34.58
	Temperature controller (reverse)	CO_2 stream temperature, °C	Condenser duty	49.95	0.18	0.999
	Duty controller (reverse)	Stripper temperature, °C	Reboiler duty	222.5	61.30	1.998

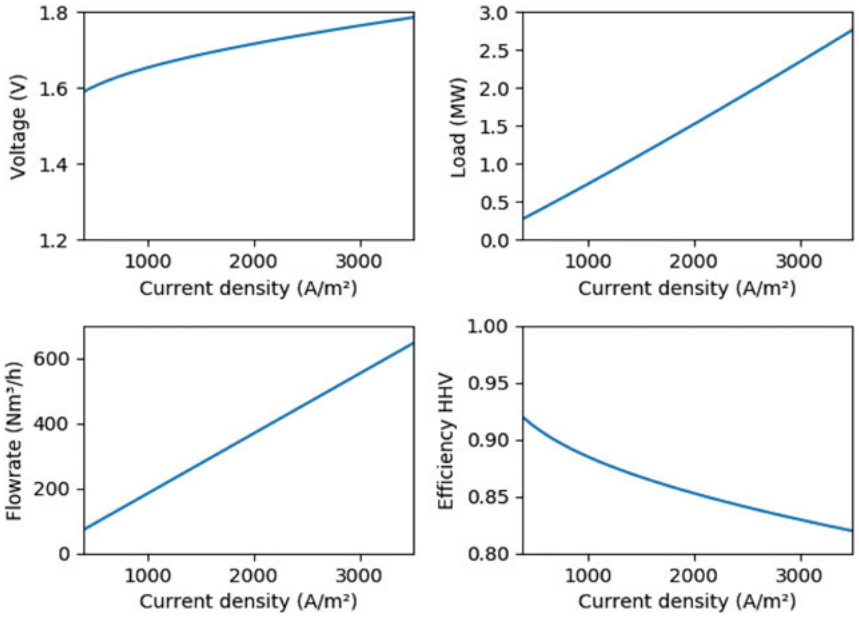

Figure 2.3: Performance of the proposed cell/stack within the operating window.

Table 2.2: Estimated parameters of AEL-stack.

Current density (i)	393.4–3500 A/m^2
Cell voltage (U)	1.59–1.79 V
Flow rate (F)	72.5–646.5 Nm^3/h
Load (W)	0.277–2.770 MW
Efficiency HHV (η)	0.92–0.82
Number of cells (N_c)	173
Peripheral load (W_p)	0.40 MW
Temperature (T)	80 °C
Pressure (P)	1.3 bar
a_1	2.72*10^{-5} V-m^2/A
B	0.118 V
c_1	5.02 m^2/A
f_1	0.94
f_2	270 A^2/m^4

restriction is on the times for restarting the operation after standby or shutdown periods. It is reported that a cold start-up takes 20 min and full start-up can take 30–60 min [12–14].

In addition to operation at full or partial loads (denoted as production state), electrolyzers can undergo a standby and idle state. The standby state refers to the load of peripheral components (pumps, heat exchangers, etc.), without charging the electrolysis cells, to keep the system operating conditions and avoiding shutdown. The idle state involves a complete shutdown of the system. Both standby and idle states present different requirements to restart the operation to production state. The states considered and transitions considered in this work are reported in previous work [11], while the model constraints are defined as follows:

– State exclusivity

$$L_{n,t} + S_{n,t} + I_{n,t} = 1, \forall n \in \{1, \ldots, N\}, \forall t \in \{1, \ldots, \tau\} \tag{2.1}$$

– Cycles count

$$I_{n,t-1} - I_{n,t} \leq Y_{n,t} \tag{2.2}$$

$$I_{n,t} - I_{n,t-1} \leq Z_{n,t} \tag{2.3}$$

$$\forall n \in \{1, \ldots, N\}, \forall t \in \{2, \ldots, \tau\}$$

– Minimum down time

$$I_{n,t-2} - I_{n,t-1} + I_{n,t} \geq 0, \forall n \in \{1, \ldots, N\}, \forall t \in \{2, \ldots, \tau\} \tag{2.4}$$

– Electrolyzer load capacity

$$\left(W^{LB} + W^{\mathrm{PC}}\right)L_{n,t} + W^{\mathrm{PC}}S_{n,t} \leq W_{n,t} \leq \left(W^{\mathrm{UB}} + W^{\mathrm{PC}}\right)L_{n,t} + W^{\mathrm{PC}}S_{n,t} \tag{2.5}$$

$$\forall n \in \{1, \ldots, N\}, \forall t \in \{1, \ldots, \tau\}$$

– Electrolyzer production rate

$$F_{n,t} = m\left(W_{n,t} - W^{\mathrm{PC}}\left(1 - I_{n,t}\right)\right) + bL_{n,t}, \forall n \in \{1, \ldots, N\}, \forall t \in \{1, \ldots, \tau\} \tag{2.6}$$

– Load ramp up-and down rates

$$W_{n,t-1} - \mathrm{RU} \leq W_{n,t} \leq W_{n,t-1} + \mathrm{RD}, \forall n \in \{1, \ldots, N\}, \forall t \in \{2, \ldots, \tau\} \tag{2.7}$$

– Load balance

$$W_{n,t} = W_{n,t}^{R} + W_{n,t}^{\mathrm{NR}}, \forall n \in \{1, \ldots, N\}, \forall t \in \{1, \ldots, \tau\} \tag{2.8}$$

– Renewable and non-renewable load capacities

$$\sum_{n=1}^{N} W_{n,t}^{R} \leq W_{t}^{\mathrm{RS}}, \forall t \in \{1, \ldots, \tau\} \tag{2.9}$$

– Product demand

$$\sum_{t=1+\left(j-1\right)\frac{\tau}{N^{\mathrm{PD}}}}^{j\frac{\tau}{N^{\mathrm{PD}}}} \sum_{n=1}^{N} F_{n,t} \geq \frac{F^{T}}{N^{\mathrm{PD}}}, \forall j \in \left\{1, \ldots, N^{\mathrm{PD}}\right\} \tag{2.10}$$

– Unit commitment

$$W_{n,t} \le W_{n+1,t}, \forall n \in \{1, \ldots, N-1\}, \forall t \in \{1, \ldots, \tau\} \tag{2.11}$$

The objective function is set to minimize the production cost of hydrogen, which is strongly affected by the electricity purchasing cost (Eq. (2.12)) and electrolyzers investment (Eq. (2.13)). Moreover, the cost of executed start-up cycles (Eq. (2.14)) and penalty cost of loading non-renewable electricity (Eq. (2.15)) are incorporated since they represent cost terms for non-steady operations and environmental performance, respectively.

$$\text{Elec}C = \sum_{t=1}^{\tau} C_t^{\text{RS}} \sum_{n=1}^{N} W_{n,t} \tag{2.12}$$

$$\text{Inv}C = N \frac{C^{\text{INV}}}{F^{\text{LT}}} \tag{2.13}$$

$$\text{Cyc}C = C^{\text{SU}} \sum_{t=1}^{\tau} \sum_{n=1}^{N} Y_{n,t} \tag{2.14}$$

$$\text{NonRC} = C^{\text{GHG}} \sum_{t=1}^{\tau} F_t^{\text{GHG}} \sum_{n=1}^{N} W_t^{\text{NR}} \tag{2.15}$$

$$\text{Obj} = \text{Elec}C + \text{Inv}C + \text{Cyc}C + \text{NonRC} \tag{2.16}$$

The description and assumed values of the model variables and parameters are listed below (Table 2.3).

2.3 Results and discussion

2.3.1 Process integration with renewable energies

Wind power with a capacity of 100 MWp is to be converted in hydrogen, over a period of one year. Additional power to the grid is used to compensate periods of scarce power and to profit from periods of low electricity cost. Such decisions are made by the implementation of the scheduling-AEL model, which has been solved iteratively for 20–34 stacks. The results of the optimizations are shown in Figure 2.4, where it can be noticed that the optimal number of electrolyzers correspond to 27 stacks.

The optimal solution indicates that it is not necessary to match the renewable power profile, but rather to balance the electricity, emissions, cycles, and investment cost. The renewable energy available in the system as well as the power load of electrolyzers is shown in Figure 2.5, while the production schedules for the electrolyzers can be observed in Figures 2.6 and 2.7 for two sample periods with full load and partial load, respectively.

Table 2.3: Nomenclature AEL-scheduling model.

b, m	Parameters of stack linear model, 19.3406 kg/MWh and 2.9634 kg/h, respectively.
C_t^E	Electricity cost (day-ahead cost) in Germany 2019 [15], in €/MWh
C^{INV}	Investment cost, 2.3 M€/electrolyzer [16]
C^{NR}	Penalty cost for the use of non-renewable power, 0.2 €/kg_{GHG}
C^{SU}	Cycles cost, approximated to 50 €/cycle
$F_{n,t}$	Hydrogen production rate, in kg/h
F_t^{GHG}	GHG emissions factor in Germany 2019 [15], in kg/MWh
F^{LT}	Lifecycle of electrolyzers, 7.5 a [16]
F^T	Hydrogen annual demand
$\mathrm{I}_{n,t}$	Idle state, binary variable
$\mathrm{L}_{n,t}$	Production state, binary variable
N	Unit index
N	Total number of units
N^{PD}	Number of equally distributed production periods, in h
$S_{n,t}$	Standby state, binary variable
T	Time index, in h
τ	Time horizon, 8760 h
$W_{n,t}$	Total power load of electrolyzers, in MW
W_{LB}, W_{UB}, W_{PC}	Minimum, maximum and peripheral load of electrolyzers, 0.6 MW, 3.3 MW, and 0.3 MW, respectively.
$W_{n,t}^{\mathrm{NR}}$	Power load from the grid (unlimited), continuous variable, in MW
$W_{n,t}^{R}$	Power load from the renewable source, continuous variable, in MW
W_t^{RS}	Renewable power capacity for simulated 100-MW wind power in northern Germany 2019 [17], in MW
$Y_{n,t}$	Start-up cycle, binary variable

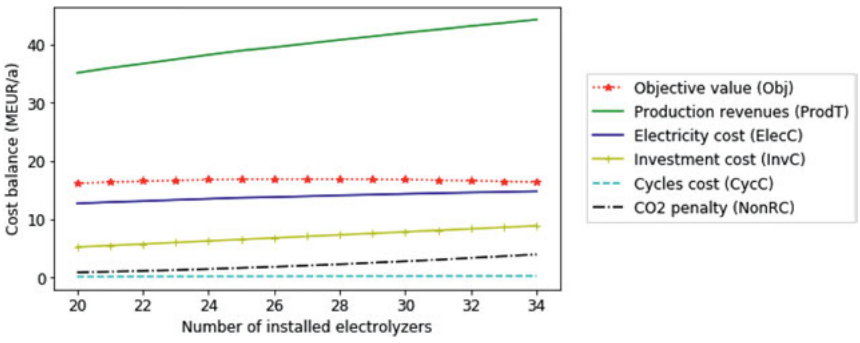

Figure 2.4: Optimal solution and influence of individual cost terms.

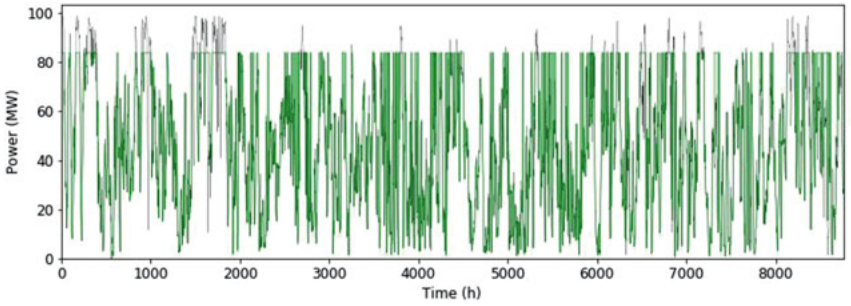

Figure 2.5: Facility load with 27 installed electrolyzers. Background in black shows the renewable power profile.

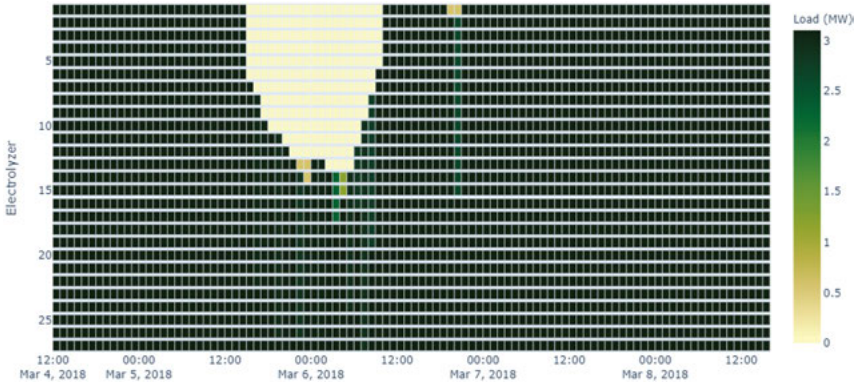

Figure 2.6: Schedule of electrolyzers with 27 installed units for the renewable case scenario. Time interval considered: 1500–1600 h.

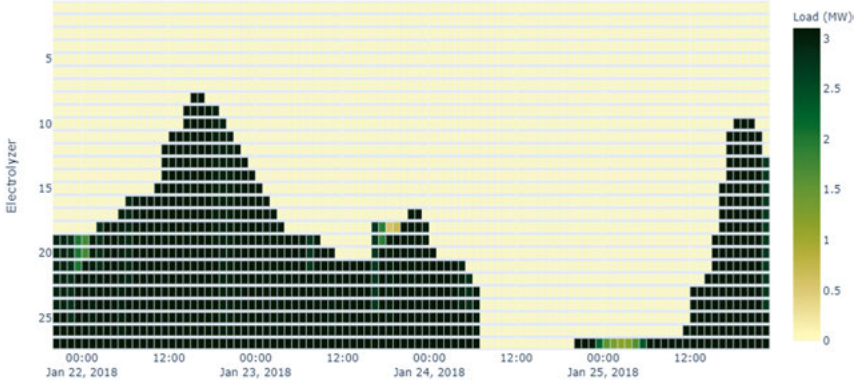

Figure 2.7: Schedule of electrolyzers with 27 installed units for the renewable case scenario. Time interval considered: 500–600 h.

The optimized operation shows that under realistic operation of electrolyzers (states and transitions), the process economics can be further improved. Although there are several fluctuations over the time horizon, the optimization model aids in deciding the optimal configuration and schedule of the P2X facility. This can be achieved by complete automation of the production units for the changes of state and load set points.

2.3.2 Process integration with electrolysis

The integration of the carbon capture and electrolysis models occurs through hydrogen production tracking. The flowrate of hydrogen has been obtained from the previous section, yet a representative 24 h scenario was extracted from the data to simulate the dynamic model of the carbon capture process in a reasonable time.

The dynamic carbon capture model has been set to follow the operation of the electrolysis stage considering a stoichiometric ratio of 1:3 for further conversion of the materials. The hydrogen-tracking scenario, shown in Figure 2.8, considers a representative 24 h period in which the fluctuations of hydrogen are around 20 MW. The dynamic operation of the carbon capture stage enables tracking the hydrogen production closely and fulfil the stoichiometric requirements for the subsequent methanol reactor.

It is also ensured that the desorber operational parameters were maintained within the desired range as shown in Figure 2.9, where 10 h of the complete run were extracted. The output pressure and temperature are within the set limits. The CO_2 stream mass fraction remains higher than 98% ensuring that the desired purity is delivered to the methanol reactor throughout the entire transient scenario.

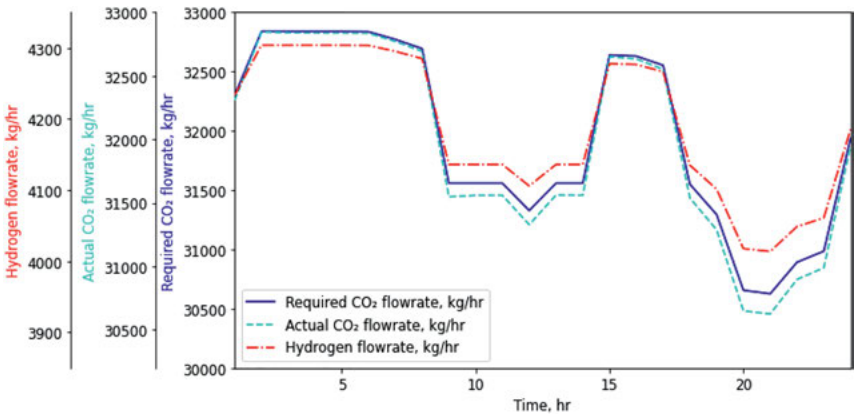

Figure 2.8: The hydrogen tracking scenario indicating the captured CO_2 flowrate.

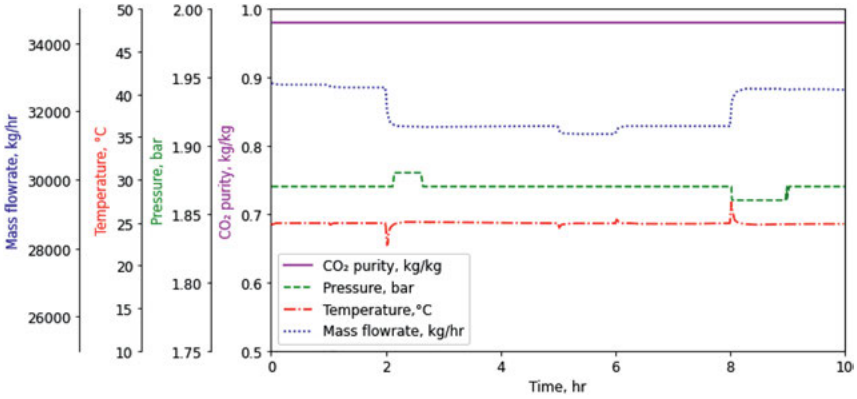

Figure 2.9: Various desorber parameters during hydrogen tracking scenario.

Through flexible operation, we are able to improve their carbon capture plant economics when retrofitted with power generation plants, as the energy penalty is not constant for the entire time duration. Power outputs could be increased during peak electricity prices by reducing the capture rate and thus increasing revenues. On the other hand, when carbon prices go high or when the carbon credits are consumed, the CC plant could be ramped up to capture more CO_2 and reduce carbon dioxide emissions, which would translate into higher carbon costs [5].

2.4 Conclusions

Models have been implemented to simulate the operation of the electrolysis and carbon capture stages of a P2X process, with a particular focus on the influence of time. This is of great interest for the efficient conversion of fluctuating renewable electricity into added-value chemicals, such as methanol.

It is observed that the electrolysis stage optimizes its production schedule to maximize the economic performance, while the carbon capture stage timely produces the required amount of carbon dioxide, keeping the ratio as the controlled variable. With the optimization of the AEL-scheduling model, the maximum profit has been determined with the flexible operation of 27 electrolyzers and 96% of renewable energy use. Furthermore, the controllers implemented at the capture stage allows for CO_2 flowrates with deviations lower than 1% within the observed 24 h interval. The operation however may be challenged-even become unfeasible-at the capture stage when considering periods with higher and more frequent fluctuations of hydrogen. Therefore, further studies should include intermediate storage of hydrogen in gas holders to reduce the disturbances at the capture process or intermediate storage of carbon dioxide in the liquid solvent.

List of Abbreviations

RES	Renewable energy sources
CC	Carbon Capture
MEA	Monoethanolamine
P2X	Power-to-X
AEL	Alkaline Water Electrolysis
NLP	Non-Linear Program
MILP	Mixed-Integer Linear Program

References

1. Bundesnetzagentur and Bundeskartellamt. Monitoring report 2018 – key findings and summary. Bonn: BUNDESNETZAGENTUR | BUNDESKARTELLAMT; 2019:1–511 pp.
2. Moseley PT, Garche J. Electrochemical energy storage for renewable sources and grid balancing. Amsterdam: Elsevier; 2015.
3. Van-Dal ÉS, Bouallou C. Design and simulation of a methanol production plant from CO_2 hydrogenation. J Clean Prod 2013;57:38–45.
4. Bellotti D, Rivarolo M, Magistri L. Economic feasibility of methanol synthesis as a method for CO_2 reduction and energy storage. Energy Proc 2019;158:4721–8.
5. Mostafa M, Varela C, Franke MB, Zondervan E. Dynamic modeling and control of a simulated carbon capture process for sustainable Power-to-X. Appl Sci 2021;11:9574.
6. Oates DL, Versteeg P, Hittinger E, Jaramillo P. Profitability of CCS with flue gas bypass and solvent storage. Int J Greenh Gas Control 2014;27:279–88.
7. Millet P, Grigoriev S. Water electrolysis technologies. Waltham: Elsevier; 2013:19–41 pp.
8. Carmo M, Stolten D. Energy storage using hydrogen produced from excess renewable electricity. London: Elsevier; 2019.
9. Ulleberg Ø. Modeling of advanced alkaline electrolyzers: a system simulation approach. Int J Hydrogen Energy 2003;28:21–33.
10. Thyssenkrupp. Hydrogen from large-scale electrolysis. Dortmund: Thyssenkrupp; 2019:8 p.
11. Varela C, Mostafa M, Zondervan E. Modeling alkaline water electrolysis for Power-to-X applications: a scheduling approach. Int J Hydrogen Energy 2021;46:9303–13.
12. Seibel C, Kuhlmann JW. Dynamic water electrolysis in cross-sectoral processes. Chem Ing Tech 2018;90:1430–6.
13. Lüke L, Zschocke A. Alkaline water electrolysis: efficient bridge to CO_2-emission-free economy. Chem Ing Tech 2020;92:70–3.
14. Ulleberg Ø, Nakken T, Eté A. The wind/hydrogen demonstration system at Utsira in Norway: evaluation of system performance using operational data and updated hydrogen energy system modeling tools. Int J Hydrogen Energy 2010;35:1841–52.
15. Agora Energiewende. Agorameter. Berlin: Agora Energiewende; 2019.
16. NOW. Studie IndWEDe. Berlin: NOW GmbH; 2018.
17. Staffell I, Pfenninger S. Using bias-corrected reanalysis to simulate current and future wind power output. Energy 2016;114:1224–39.